Significant Findings Statement

35 GHz Measurements of CO_2 Crystals for Simulating Observations of the Martian Polar Caps

J. L. Foster, A. T. C. Chang, D. K. Hall, A. B. Tait, and J. S. Barton

Question: Using a 35 GHz hand-held radiometer, do dry ice (CO_2) crystals scatter and absorb passive microwave energy similarly to that of snow (H_2O) crystals?

Approach: In this experiment, passive microwave radiation emanating from within a 33 cm snowpack was measured with a 35 GHz hand-held radiometer, and in addition to the natural snow measurements, the radiometer was used to measure the microwave emission and scattering from layers of manufactured CO_2 (dry ice). A 1 m x 2 m plate of aluminum sheet metal was positioned beneath the natural snow so that microwave emissions from the underlying soil layers would be minimized. Different layers of the snow and the dry ice were removed and the measurements were repeated.

Significance: This study demonstrates that the dry ice brightness temperatures were considerably lower than those of the snow crystals for two primary reasons. One, the dry ice crystals were an order in magnitude larger than the snow crystals, and two, they were significantly colder than the snow crystals. Large crystals, which approach the wavelength size of the sensor, are very effective scatters of microwave radiation. The colder physical temperature of the dry ice crystals also contributes to the lower brightness temperatures.

Mars Polar Science Special Issue

35 GHz Measurements of CO_2 Crystals for Simulating Observations of the Martian Polar Caps

J. L. Foster*, A. T. C. Chang*, D. K. Hall*, A. B. Tait**, and J. S. Barton***

***Hydrological Sciences Branch, Laboratory for Hydrospheric Processes,**

NASA/Goddard Space Flight Center, Greenbelt, Maryland 20771

**** Universities Space Research Association, Lanham, Maryland 20706**

***** General Sciences Corporation, Beltsville, Maryland 20770**

James Foster, Phone: 301-614-5769, Fax: 301-614-5808,

email: jfoster@glacier.gsfc.nasa.gov

25 manuscript pages, 3 tables and 4 figures
key words: ices, Mars surface, Mars climate, Earth

35 GHz measurements of CO_2 crystals

Editorial correspondence should be directed to

James Foster
NASA/GSFC
Code 974
Greenbelt, MD 20771

ABSTRACT

In order to learn more about the Martian polar caps, it is important to compare and contrast the behavior of both frozen H_2O and CO_2 in different parts of the electromagnetic spectrum. Relatively little attention has been given, thus far, to observing the thermal microwave part of the spectrum. In this experiment, passive microwave radiation emanating from within a 33 cm snowpack was measured with a 35 GHz hand-held radiometer, and in addition to the natural snow measurements, the radiometer was used to measure the microwave emission and scattering from layers of manufactured CO_2 (dry ice). A 1 m x 2 m plate of aluminum sheet metal was positioned beneath the natural snow so that microwave emissions from the underlying soil layers would be minimized. Compared to the natural snow crystals, results for the dry ice layers exhibit lower microwave brightness temperatures for similar thicknesses, regardless of the incidence angle of the radiometer. For example, at 50° H (horizontal polarization) and with a covering of 21 cm of snow and 18 cm of dry ice, the brightness temperatures were 150 K and 76 K, respectively. When the snow depth was 33 cm, the brightness temperature was 144 K, and when the total thickness of the dry ice was 27 cm, the brightness temperature was 86 K. The lower brightness temperatures are due to a combination of the lower physical temperature and the larger crystal sizes of the commercial CO_2 crystals compared to the snow crystals. As the crystal size approaches the size of the microwave wavelength, it scatters microwave radiation more effectively, thus lowering the brightness temperature. The dry ice crystals in this experiment were about an order of magnitude larger than the snow crystals and three orders of magnitude larger than the CO_2 crystals produced in the cold stage of a scanning electron microscope. Spreading soil, approximately 2 mm in thickness, on the dry ice appeared to have no effect on the brightness temperatures.

Key words: ices, Mars surface, Mars climate, Earth.

1.0 Introduction

The most recent measurements made from the Mars Global Surveyor Mission using laser altimetry methods (Mars Orbital Laser Altimeter, MOLA), indicate that the residual northern cap of Mars has an average thickness of 1.03 km and may have a maximum thickness of 3 km (Smith et al., 1998; Zuber et al., 1998). For the seasonal pack, the thickness may be about 1 m at higher latitudes (north of 60 degrees). Although at lower latitudes (50-60 degrees), or near the southern margin of the cap, the accumulation is possibly less than 1 cm. Hess et al. (1979) have estimated that the thickness of the seasonal snow layers (consisting of frozen H_2O and frozen CO_2) to be a few tens of centimeters. If this is so, the thickness is only somewhat less than terrestrial accumulations of seasonal snow, which at sea level rarely exceed a meter over extended areas.

In terms of remotely sensing the Martian seasonal and permanent ice caps, relatively little attention has been thus far given to observing the thermal microwave part of the spectrum. The microwave region contributes little to the total radiation budget of Earth or Mars, compared to the ultraviolet, visible and infrared wavelengths. However, because ice crystals appreciably scatter and absorb (depending on the crystal size) upwelling microwave radiation emanating from the Earth at frequencies above about 10 GHz, microwave radiometry offers the potential to assess the thickness and the extent of the Martian seasonal caps using remote sensing techniques. An advantage of using this approach is that microwaves are indifferent to daylight and darkness. Therefore, the

thickness and extent of the caps can be estimated even during the polar night period. (Foster et al., 1998).

Although much of what is known about the composition and structure of the Martian polar caps is a result of laboratory work and modeling, in the microwave region of the spectrum, there is a need to conduct basic experiments related to how microwaves are scattered and or absorbed by accumulations of CO_2 crystals having various sizes. A problem, of course, with experimental measurements, is how to make them under conditions which are analogous to the conditions expected on Mars. Otherwise, the results may not fully explain what is observable on Mars. Nonetheless, initial experiments with preliminary findings are useful for helping to design further experiments and to validate modeling results.

The purpose of this paper is to measure the passive microwave brightness temperatures at 35 GHz (~0.8 cm), using a hand-held radiometer, of dry ice crystals and to compare these measurements with snow (H_2O) measurements. The CO_2 brightness temperatures will be modeled, using a discrete dipole scattering model, and compared to the radiometric observations. Unfortunately, there are no direct (in situ) Viking Lander measurements of the Martian polar caps, and there are few orbital measurements (either from the Mariner, Mars, Phobos or even Pathfinder missions), that can be used as a standard of reference for comparison with the laboratory measurements of CO_2 crystals and the modeling results on CO_2 extinction efficiency described in this paper. However, the measured response from

dry ice can be compared with the modeled results to assess whether or not the model can be used to accurately gage the extinction of CO_2 and H_2O crystals having different sizes.

2.0 Passive Microwave Radiometry

The microwave radiation emitted by a covering of H_2O or CO_2 snow is dependent upon the physical temperature, crystal characteristics and the density of the snow. A basic relationship between these properties and the emitted radiation can be derived by using the radiative transfer approach. The lack of precise information about crystal size, shape and the snowpack density is compensated for by using averages for these parameters, based on field and laboratory observations. For computational purposes, assumptions are made that the averages are representative of conditions encountered throughout the snowpack. These quantities are then used as input to radiative transfer equations to solve the energy transfer through the snow covering. If the assumptions about the averages differ substantially from actual observations, then poor values of the thickness of the covering, or in the case of snow, the snow water equivalent will result (Foster et al. 1998).

Microwave emission from a snow layer over a ground medium consists of contributions from the snow itself and from the underlying ground. Both contributions are governed by the transmission and reflection properties of the air-snow and snow-ground boundaries and by the absorption/emission and scattering properties of the snow layers. If the snowpack is thick (> penetration depth of the wavelength) then it may be treated as a semi-infinite medium and contributions from the ground will not be as important (Chang et al., 1976).

As an electromagnetic wave emitted from the underlying ground propagates through the snowpack, it is scattered by the randomly-spaced snow particles in all directions. Consequently, when the wave emerges at the snow/air interface, its amplitude has been attenuated, and thus the brightness temperature is low. Dry snow absorbs very little microwave energy, and therefore it contributes very little in the form of self-emission (Ulaby and Stiles, 1981; Foster et al., 1984). For snowpacks on Earth, snow crystals are effective scatterers of microwave energy for frequencies greater than about 10 GHz. The snow crystals redistribute part of the cold sky radiation, which reduces the upwelling radiation measured with a radiometer (Schmugge, 1980). The deeper the snow, the more snow crystals are available to scatter the upwelling microwave energy, and thus it is possible to estimate the depth of the snow and the snow water equivalent.

The difference in brightness temperature between the18 GHz and the 37 GHz microwave frequencies has been used to derive snow depth for a uniform snowfield. The Chang et al. (1987) algorithm is expressed as follows:

$$SD = C\,(T18 - T37)$$

where SD is snow depth in centimeters, T is the brightness temperature in degrees K and C is a coefficient related to grain size. If $T18 < T37$, the snow depth is zero.

An evaluation of the various algorithms that have been used to derive snow parameters shows that only those algorithms including 37 GHz frequencies provide adequate agreement with the manually measured snow depth values. Use of the 18 GHz frequency helps to eliminate the effects of the snow and ground temperatures and the atmospheric quantities (integrated water vapor and clouds) on changes in T (Chang et al., 1987).

How closely packed the particles are to each other (density) is related to the path length of the radiating energy, and is thus important in terms of scattering potential. While field measurements of snow density are routinely made, this parameter is difficult to extract using remote sensing technology. A representative value of 300 kg m^{-3} is typically assumed in developing algorithms for mid-latitude snowpacks in mid-winter (Foster et al. 1998). This value varies in response to the water content of the snow, and thus it can change (increase) even if the depth of the snowpack remains fairly constant. For CO_2 snowpacks, a density value of about 1067 kg m^{-3} has been estimated by a number of authors, including Yamada and Person (1964), Seiber et al. (1971), and (Tsujimoto et al. (1983).

Large snow crystals are especially effective scatters of microwave energy (Hall, et al., 1986; Armstrong et al., 1993). Foster et al. (1997) have shown that for snow, the shape of the crystal is insignificant, in comparison to the size of the crystal and the spacing between the crystals, in scattering the microwave radiation emanating from the ground and passing through the snowpack. In the above equation "C" will be smaller with a larger crystal

size. For example, if the average crystal radius is 0.3 mm, C is 1.59, and if the radius is 0.5 mm, C is 0. 39 (Foster et al. 1998).

For H_2O ice, the complex index of refraction is 1.78 for the real part and 0.0024 for the imaginary part (Chang et al., 1987). Absorption of microwave energy by dry snow crystals is very small, about 10^5 times smaller than for water in the liquid phase (Ulaby and Stiles, 1981).

Only a few measurements are available of either the dielectric or the refractive index for frozen CO_2 ; for example Seiber et al. (1971), Warren (1986) and Hansen (1997) or for clathrate ices (Gough and Davidson, 1973). In the microwave portion of the spectrum, Simpson et al. (1980) obtained a dielectric constant of 2.25 for frozen CO_2 in the frequency range between 2.2 and 12 GHz, for a density of 1400 kg m^{-3} and for temperatures between 113 and 183 K. Estimating an uncertainty of about 10% in their value for the dielectric constant, gives a refractive index of 1.5 (+ or - 0.1). The loss tangent, represented by the imaginary part of the refractive index, is listed as < 0.004 throughout this same frequency range. The same authors made less accurate measurements for both the real and imaginary part of the index of refraction, out to 50 MHz which suggest that the above values are valid (Warren, 1986). For temperatures greater than 77 K, Warren (1986) showed that away from the absorptive bands, the refractive index varies only from 1.40 at 1 μm to 1.44 at microwave frequencies. At 1000 GHz, Hansen gets a real value of 1.444 and an imaginary value of 0.0048 (Hansen, 1997). Because no Debye relaxation absorption is expected in the microwave region, the

imaginary index should be very low since CO_2 is not a polar molecule (Hansen, personal communication).

Methodology

An out-of-doors site was deemed necessary for this experiment because the numerous thermal emission sources in an indoor cold laboratory (walls, tables, etc.) would contaminate the microwave measurements. Measurements were made in the northern plains of North Dakota during the week of February 8, 1998 at a site near Grand Forks, North Dakota. Though the snowpack exceeded 30 cm at the site we selected, and the temperatures were below 0 ° C, for this time of year in North Dakota, the snowpack thickness was below normal and the weather conditions were mild. The underlying vegetation consisted of a mixture of grasses. At the time of the experiment, the sky was in complete overcast, but no precipitation was reported.

To conduct this experiment we required approximately 300 lbs of dry ice pellets which were purchased from a nearby commercial supplier. This type of commercially available frozen CO_2 is produced by compressing and then rapidly expanding CO_2 gas. Liquid CO_2 is allowed to expand by reducing its pressure to sea level atmospheric pressure (~1013 mb). This spontaneously converts the liquid to both a gas and a solid. If the expansion occurs in a cold chamber, the snow, which represents approximately 40% of the liquid conversion, can be compacted to conform to the chamber shape and size. The most common forms of manufactured dry ice are pellets and solid blocks.

A 1 m by 2 m plate of aluminum sheet metal was positioned beneath the natural snow so that microwave emissions from the underlying soil layers would be minimized. 35 GHz measurements of this plate were made through the 33 cm snowpack (Figure 1). Measurement units are in volts. Voltages were later converted to brightness temperatures. Natural snow layers, corresponding to snowfalls earlier in the season, were removed and measurements were repeated for the diminishing snowpack until the bare sheet metal plate was in view. Then, 9 cm of CO_2 crystals were deposited onto the plate, and as was the case for the natural snow, hand-held measurements were made each time the thickness of the deposit was altered. These CO_2 crystals were approximately 0.60 cm in diameter and were cylindrical in shape (Figure 2). The temperature of the dry ice was -76 ° C, whereas the temperature at the top of the snowpack was -1.9 ° C (the air temperature was -3 ° C). Two additional 9 cm increments were placed on top of the existing CO_2 crystals, resulting in a total thickness of 27 cm of dry ice. Because of the difficulty of working with the dry ice pellets, it was decided that three separate 9 cm deposits of the dry ice would be made rather than trying to match the exact thickness of the natural snow layers.

After this series of measurements was made, the CO_2 crystals were then placed on top of the snowpack, and as before, measurements were made using the 35 GHz radiometer. As a final part of this experiment, soil particles were spread on top of the dry ice, and once again, microwave measurements were made with the 35 GHz radiometer. Selected hand-held radiometer measurements are shown in Table I.

The natural dry ice crystal shape is typically pseudo-octahedral, where two four-sided pyramids share a common base. Specifically this type of crystal is known as a tetragonal - ditetragonal bipyramid. Although the dry ice crystals used in this experiment were manufactured to be in the shape of cylindrical pellets, the shape of the crystal has been shown to have little effect on microwave scattering (Foster et al., 1997).

4.0 Modeling

Modeling provides a means to gage the efficacy of using passive microwave remote sensing to estimate CO_2 thickness. As mentioned previously, it is impractical to use a microwave radiometer to make measurements in a laboratory setting because background emission would corrupt the measurements.

A particle scattering model was used to assess the scattering properties of the large dry ice pellets. In this experiment, crystals were modeled having an effective radius (radii of a sphere of equal volume) of 500, 1,000, 5,000, and 10,000 μm (0.6 cm). The discrete dipole scattering (DDSCAT) model employed here is a Fortran program which calculates scattering and absorption of electromagnetic radiation by arbitrary targets using the discrete dipole approximation (DDA). With this approximation, the targets are replaced by an array of point dipoles. The electromagnetic scattering problem for the arrays is then solved, essentially exactly (Draine, 1988 and updated in Draine and Flatau, 1994; Foster et al., 1997).

According to Draine (personal communication) DDSCAT can be used for any isotropic material. Even if the material is anisotropic, it can be used providing that certain dielectric tensor conditions are satisfied. For best results, the dielectric constant should not be too large ($< \sim 4$). DDSCAT is a versatile program and has been used to address scattering from materials such as snow, ammonia or interstellar dust (Draine, 1988; West et al., 1989). The program code incorporates Fast Fourier Transform methods (Goodman et al., 1991).

For this investigation, the wavelength chosen is 8500 μm (0.85 cm), corresponding to a frequency of 35 GHz. It has been demonstrated (Chang et al., 1987) that for a snowpack less than a meter in depth, more information about the snow water equivalent and thickness can be derived when using a frequency of about 35 GHz than when using higher or lower frequencies. For the refractive index of frozen CO_2, a value of 1.42 was used for the real part and 0.005 was used for the imaginary part. Three different target orientations with calculations for two incident polarizations states are available with this model. Here, randomly oriented dipoles are specified. Scattering intensities are computed for two scattering planes at intervals of 30 degrees in the scattering angle theta; phi = 0 for the x-y plane, and phi = 90 for the x-z plane. The true thickness of a deposit is not required for emission boundary conditions; scattering or absorption results from the array of point dipoles (Foster et al., 1998).

Table II gives values for extinction, absorption and scattering efficiency of frozen carbon dioxide crystals for different particle sizes using a frequency of 35 GHz and a refractive

index of 1.44 + .0005 (Hansen, personal communication). For comparison purposes, Table III gives extinction, absorption and scattering values, as modeled for H_20 crystals. This comparison is shown as a plot in Figure 3.

5.0 Discussion

For small crystals, such as those produced in the cold stage of a scanning electron microscope (SEM), it has been shown by Foster et al. (1998) that for the smallest particles (< ~ .300 mm), absorption values are greater than are scattering values at the microwave frequencies. For this experiment, the dry ice crystals were three orders of magnitude larger than the ones produced in the cold stage of the SEM. Although, not shown here, only small differences exist for the various particle shapes (other than those than in Tables II and III) and orientations as well.

The size of the crystal affects scattering considerably more than it does absorption, at a frequency of 35 GHz, for both CO_2 and H_2O crystals. Scattering dominates over absorption for the larger sizes of the modeled crystals since the particles approach the size of the wavelength (Mie scattering). For instance, the scattering values are an order of magnitude larger than absorption for the range of H_2O particles listed in Table III.

Referring to Figure 3, notice, however, that extinction decreases with crystal size for the largest crystals (10,000 μm). According to Tables II and III, extinction, absorption and scattering each decrease from 5,000 μm to 10,000 μm. This is especially noticeable for the

tetrahedron crystals (Table II). When the particle size is greater than the wavelength (8,100 μm), extinction no longer increases but rather oscillates (Ulaby at al, 1981). Calculations of the attenuation cross sections of large ice and water spheres have shown that the normalized attenuation cross section increases up to a size parameter (α) of 1, and then from there decreases to a size parameter of 5 (Atlas and Wexler, 1963; Battan, Browning and Herman, 1970).

Compared to natural snow crystals, the dry ice crystals exhibited lower brightness temperatures. This is attributed to 1) greater scattering effects and 2) colder physical temperatures of the dry ice. Because the dry ice crystal sizes are about an order of magnitude larger than the largest snow crystals, the scattering is greater and hence the brightness temperatures are lower. For instance, with a thickness of 21 cm of snow on the aluminum plate and with an incidence angle of 50 degrees (horizontal polarization), the brightness temperature was 150 K, whereas for the dry ice, the brightness temperature registered 76 K with a thickness of 18 cm on the plate. For a depth of 33 cm of snow, the brightness temperature was 144 K. This compares to a brightness temperature of 86 K when 27 cm of dry ice was placed on top of the aluminum plate. The physical temperature of the snow surface was – 3 ° C, however, the temperature of the dry ice was –76 ° C. Since brightness temperature is a function of both the emissivity and physical temperature of a material, the colder temperature of the dry ice accounts for some of the difference in the brightness temperature between the water snow and CO_2 snow.

Figure 4 shows the 35 GHz brightness temperatures of both water and CO_2 snow for various depths over the aluminum plate. Notice that for the water snow, the brightness temperatures decrease between depths of 33 cm and 21 cm – when the snow surface was measured at its full depth and then again when 9 cm were removed from the top of the pack. This is probably a result of the frozen nature of this uppermost snow layer. Melt and freeze events occurring several weeks after snow had fallen to form this layer, resulted in the formation of a surface crust (ice lens), which acted not to scatter the passive microwave radiation but to absorb it instead.

It should also be pointed out that the brightness temperature of the dry ice decreases gradually with increasing thickness. From 27 cm to 9 cm the TB decreases by only 32 ° K (< 2 degree K per cm). This demonstrates that the temperature of the dry ice is largely responsible for the low TBs, otherwise volume scattering by the large dry ice crystals would significantly lower the TB with increasing thickness. For particles the size of the dry ice crystals used in this experiment, nearly all of the scattering would be expected to occur in the upper 0.5 meter of the snowpack (either CO_2 or H_2O snowpacks).

On Mars, even though frozen CO_2 is isothermal, gradients could exist between the surface (ground) and the overlying-layer of the seasonal CO_2 snowpack and between the CO_2 snowpack and the atmosphere. Because much of the atmospheric CO_2 is depleted when frozen CO_2 exists on the surface, the vapor pressure gradient may be sufficiently large so as facilitate the growth of larger crystals. In the 2.0 - 4.0 μm part of the spectrum, reflectance models by Calvin (1990) and Calvin and Martin (1994), and albedo models by

Hansen and Martin (1993) show that equivalent CO_2 grain sizes may be very large, on the order of a few mm to a cm, and that polar cap spectra in this wavelength range are dominated by absorption. In the microwave region, such large crystals would dominate scattering and cause lower than expected brightness temperatures (Foster et al., 1998).

In order to derive a reliable measure for the thickness of CO_2 deposits by utilizing passive microwave techniques, either the size of the scatterers or the density of the CO_2 snowpack must be known with a high degree of accuracy. Geographic location, the time of year, elevation, and wind are several of the many controls affecting crystal size and density. From the above discussion, it is likely that the CO_2 crystals on the surface of Mars range in size from microns to millimeters. It may be possible to retrieve more precise grain size information for the polar caps of Mars using laser altimetry (from MOLA). Because both H_2O and CO_2 reflectance is sensitive to grain size at the MOLA wavelengths, the potential exists to determine the sizes of water ice and carbon ice grains (Nolin, 1998).

On Earth, the density is greater in regions where the mean wind velocities are higher because winds promote saltation, which causes the edges and ends of the crystals to break off. The result being that the particles are more spherical and smaller, and thus packing is more easily facilitated. For example, Grenfell and Warren (1994) have shown that the snow grain sizes (radii) near the South Pole in Antarctica are typically less than 0.150 mm, at depths 10 cm below the surface. Recall that for a mid-winter mid-latitude snowpack, grain sizes are on average approximately 0.3 mm.

This may be the case on Mars as well, however, the low atmospheric density, and the fact that CO_2 crystals are not dendritic (they do not have a large number of protuberances which can be easily worn down) may keep snowpack densities on Mars from increasing appreciably as the winter season progresses. Additionally, lack of a liquid phase on Mars prevents density from increasing in the spring period, as it does for snowpacks on Earth.

It may be found that specific geographic or climatic regions on Mars have a predisposition for having crystals with certain sizes and densities. For example, near the margins of the northern cap, the thickness of the pack is estimated to be on the order of millimeters. Because the thickness along the margins or boundaries of a snowcap are expected to be small, it is probable that the particle size and density in these locations will be similar from one year to another, even if the boundary itself has migrated somewhat over a period of several years. Therefore, regardless of the amount of variation that exists in particle size and density globally on Mars, there is a potential for developing algorithms which are applicable for specific regions.

As discussed in Foster et al. (1998), if the Martian polar caps are annealed or at least partially annealed, volume scattering by discrete particles (snow crystals) would not apply. For conditions analogous to the polar firn in Greenland and Antarctica, where there may be tens or hundreds of dense horizontal layers, each a few centimeters thick and characterized by its own density, temperature and grain size distribution, the use of dense media models prove to be more reliable in modeling the emerging microwave radiation and in thus, estimating the thickness (Tsang and Ishimaru, 1985; West, 1994). Dense

media microwave scattering (at 37 GHz) is sensitive to both volume inhomogeneities, such as ice grains, and to abrupt changes in the dielectric constant at the interfaces between layers with differing densities (Matzler, 1987).

Finally, in our admittedly rather feeble attempt to simulate a sullied Martian snowpack, a thin layer of soil particles (approximately 2 mm thick) were scattered on top of the heap of CO_2 crystals. It can be seen from Table I that this was of little consequence to the microwave brightness temperatures. In the microwave portion of the spectrum, dry soil has a high emissivity and refractive index compared to that of snow. The volume of snow crystals (whether composed of H_2O or CO_2), and the resulting scattering of microwave energy, overwhelms the emission from the thin layer of soil particles added to the top of the snowpack.

5.0 Conclusions and Future Plans

In this study it was found that compared to natural snow crystals, the dry ice crystals exhibited lower brightness temperatures. This is attributed to both the greater scattering of the larger CO_2 crystals, which are about an order in magnitude larger than the largest snow crystals, and the colder physical temperatures of the dry ice. For instance, with a thickness of 33 cm of snow over an aluminum plate and with an incidence angle of 50 degrees (horizontal polarization), the brightness temperature was 144 K, whereas for the dry ice, the brightness temperature registered 86 K with a thickness of 27 cm over the plate.

During the winter of 1999, and again in 2000, similar experiments will be conducted but with differently-sized CO_2 crystals. Our intent is to mass- produce crystals smaller (< 5 mm in radius) than the manufactured dry ice used in this study. We would like to be able to construct an artificial CO_2 snowpack having larger crystals at the bottom and smaller crystals at the surface. It would be useful to measure crystals of various sizes with the 35 GHz hand-held radiometer and, in addition, to use another radiometer tuned to a higher (85 GHz) frequency.

Acknowledgements: The authors would like to thank Dr. Andrew Klein, Mr. Eric Erbe, and Dr. Paul Todhunter for assisting with the experiment and Dr. Marla Moore for her helpful comments and suggestions.

References

Armstrong, R., A. Chang, A. Rango, and E. Josberger, "Snow depth and grain size relationships with relevance for passive microwave studies" Annals of Glaciology, Vol. 17, 171-176, 1993.

Atlas, D., and R. Wexler, "Backscatter by oblate ice spheroids" Journal of Atmospheric Science, Vol. 20, 48-61,1963.

Battan, L. J., S. R. Browning and B. M. Herman, "Attenuation of microwave by wet ice spheres" Journal of Applied Meteorology, Vol. 9, 832-834, 1970.

Calvin, W., "Additions and corrections to the absorption coefficients of CO_2 ice: Applications to the Martian south polar cap" Journal of Geophysical Research Vol. 95, 14743-14750, 1990.

Calvin, W. and T. Z. Martin, "Spatial variability in the seasonal south polar cap of Mars" Journal of Geophysical Research Vol. 99, 21143-21152, 1994.

Chang, A. T. C., P. Gloersen, T. Schmugge, T. Wilheit, and H. J. Zwally, "Microwave emission from snow and glacier ice" Journal of Glaciology, Vol. 16, 23-39, 1976.

Chang, A.T.C., J.L. Foster and D.K.Hall, "Nimbus-7 SMMR derived global snow cover parameters" Annals of Glaciology, Vol. 9, 39-44, 1987.

Draine, B., 1988, " The discrete dipole approximation and its application to interstellar graphite grains" Journal of Astrophysics, Vol. 33, 848-872, 1988.

Draine, B., personal communication, 1998.

Draine, B. and P. Flatau, "Discrete dipole approximation for scattering calculations" Journal of the American Optical Society, Vol. 11, 1491-1499, 1994.

Foster, J. L., D. K. and A. T. C. Chang, "An overview of passive microwave snow research and results", Reviews of Geophysics and Space Physics Vol. 22, 195-208, 1984.

Foster, J., D. Hall, A. Chang, A. Rango, W. Wergin, and E. Erbe, "Snow crystal shape and microwave scattering" Proceedings of the IGARSS 1997, Vol. 2, 625-627, Singapore, 1997.

Foster, J., A. Chang, D. Hall, W. Wergin, E. Erbe, and J. Barton, "Carbon dioxide crystals: An examination of their size, shape and scattering properties at 37 GHz and comparisons with water ice (snow) measurements " Journal of Geophysical Research – Planets, Vol. 103, No. E11, 25,839-25,850, 1998.

Gough, S. R. and D. W. Davidson, "Dielectric properties of clathrate ices" in Physics and Chemistry of Ice Ed., E. Whalley, S. Jones and W. Gold, Royal Society of Canada, Ottawa, 51-55, 1973.

Goodman, J., B. Draine, and P. Flatau, P., "Applications of FFT techniques to the discrete dipole approximation" Optical Letters, Vol. 16, 1198-1200, 1991.

Grenfell, T. C. and S. G. Warren, "Reflection of solar radiation by the Antarctic snow surface at ultraviolet, visible and near-infrared wavelengths" Journal of Geophysical Research, Vol. 99, No. D9, 669-684, 1994.

Hall, D. K., A. T. C. Chang and J. L. Foster, "Detection of the depth hoar layer in the snow-pack of the Arctic coastal plain of Alaska" Journal of Glaciology , Vol. 32, 87-94, 1986.

Hansen, G. B., and T. Z. Martin, "Modeling the reflectance of CO_2 frosts with new optical constants: Applications to Martian south polar cap spectra" Lunar Planet Science XXIV, 601-602, 1993.

Hansen, G. B., "The infrared absorption spectrum of carbon dioxide ice from 1.8 to 333 μm" Journal of Geophysical Research Vol. 102, 21569-21587, 1997.

Hansen, G. B., (personal communication, 1998).

Hess, S. L., R. M. Henry, and J. E. Tillman, 'The seasonal variation of atmospheric pressure as affected by the south polar cap" Journal of Geophysical Research, Vol. 84, 2923-2927, 1979.

Matzler, C., "Applications of the interactions of microwaves with the natural snow cover" Remote Sensing Reviews , Vol. 2, 259-387, 1987.

Nolin, A. W., "Mapping the Martian polar ice caps: Applications of terrestrial optical remote sensing methods" Journal of Geophysical Research – Planets, Vol. 103, No. E-11, 25,851-25,864, 1998.

Schmugge, T., "Techniques and applications of microwave radiometry" in Remote Sensing of Geology, edited by B. Siegal and A. Gillespie, John Wiley, New York, chapter11, 337-352, 1980.

Seiber, B. A., A. M. Smith, B. E. Wood, and P. R. Mueller, "Refractive indices and densities of H_2O and CO_2 Films condensed on cryogenic surfaces" Applied Optics Vol. 10, 2086-2096, 1971.

Simpson, R. A., B. C. Fair, and H. T. Howard, "Microwave properties of solid CO_2" Journal of Geophysical Research, Vol. 85, no. B10, 5481-5484, 1980.

Smith, D. E, M. T. Zuber and ten others, "Topography of the northern hemisphere of Mars from the Mars Orbiter Laser Altimeter" Science, Vol. 279, 1686-1692, 1998.

Tsang, L. and A Ishimaru, "Radiative and cyclical transfer equations for dense non-tenuous media" Journal of the Optical Society of America , Vol. 2, 2187-2194, 1985.

Tsujimoto, S., A. Konishi, N. Tereda, and K. Kunimoto, "Optical constants and thermal radiative properties of CO_2 cryodeposit" Cryogenics, 251-257, 1983.

Ulaby, F. T. and W. H. Stiles, "The active and passive microwave response to snow parameters" Journal of Geophysical Research, Vol. 85, 1045-1049, 1981.

Warren, S. G., "Optical constants of carbon dioxide ice" Applied Optics Vol. 25, 2650-2674, 1986.

West, R. A., G. S. Orton, B. T. Draine, and E. A. Hubbell, "Infrared absorption features for tetrahedral ammonia ice crystals" Icarus , Vol. 80, 220-223, 1989.

West, R. D., "Microwave emission from polar firn" Ph.D. Thesis, University of Washington, 85 pages, 1994.

Yamada H. and W. Person, "Absolute infrared intensities of the fundamental absorption bands in solid CO_2 and N_2O" Journal of Chemical Physics Vol. 41, no 2, 2478-2487, 1964.

Zuber, M. T., D. E. Smith and nineteen others, "Observations of the north polar region of Mars from the Mars Orbiter Laser Altimeter" Science, Vol. 282, 2053-2060, 1998.

List of Tables

List of Figures

TABLE 1

Dry Ice Experiment
February 1998
Grand Forks, North Dakota
Open site – short grass prairie
Skies are overcast
Air temperature = -3.0°C
Snow temperature = -1.9°C

Stage 1
Sheet metal plates are inserted under the snowpack.
Snow depth = 33cm
TB_N = 145.2K N=nadir
TB_{50H} = 144K
TB_{50V} = 153K
TB_{30H} = 128.4K
TB_{30V} = 150K

Stage 2
A layer of snow is removed.
Snow depth = 20cm
TB_N = 155.4K
TB_{50H} = 150K
TB_{50V} = 156K
TB_{30H} = 140.4K
TB_{30V} = 145.2K

Stage 3
Another layer of snow is removed.
Snow depth = 6cm
TB_N = 96.6K
TB_{50H} = 105.6K
TB_{50V} = 117.6K
TB_{30H} = 97.2K
TB_{30V} = 97.2K

Stage 4
All the snow is removed (metal plates are showing).
Snow depth = 0cm
TB_N = 16.2K
TB_{50H} = 19.8K
TB_{50V} = 25.2K
TB_{30H} = 9K
TB_{30V} = 12K

Stage 5
Dry ice pellets are added onto the plates.
Dry ice temperature = -76°C
Dry ice depth = 9cm
TB_N = 75K
TB_{50H} = 57.6K
TB_{50V} = 61.2K
TB_{30H} = 60.6K
TB_{30V} = 59.4K

Stage 6
More dry ice is added.
Dry ice depth = 18cm
TB_N = 89.4K
TB_{50H} = 75.6K
TB_{50V} = 81.6K
TB_{30H} = 75K
TB_{30V} = 79.2K

Stage 7
More dry ice is added.
Dry ice depth = 27cm
TB_N = 96.6K
TB_{50H} = 85.8K
TB_{50V} = 90K
TB_{30H} = 83.4K
TB_{30V} = 83.4K

Stage 8
Dry ice pellets placed on top on an undisturbed snowpack nearby (snow depth = 23cm, dry ice depth = 18cm).
TB_N = 199.8K
TB_{50H} = 178.8K
TB_{50V} = 191.4K
TB_{30H} = 191.4K
TB_{30V} = 192.6K

Stage 9
Soil is scattered on top of the dry ice.
TB_N = 204K
TB_{50H} = 179.4K
TB_{50V} = 188.4K
TB_{30H} = 189K
TB_{30V} = 195K

Table 2
Extinction Efficiency, absorption, and scattering for carbon dioxide crystals.
The refractive index is 1.44+0.005i and the wavelength is 0.81 cm (35 GHz)

Size Parameter (α) = $2\pi r/\lambda$					
Size (μm)	Shape	Size Param.	Q_ext	Q_abs	Q_sca
500	Cylinder	0.388	8.089E-03	4.182E-03	3.907E-03
500	Sphere	0.388	8.631E-03	4.388E-03	4.242E-03
500	Tetrahedron	0.388	9.541E-03	4.828E-03	4.713E-03
1000	Cylinder	0.776	6.568E-02	9.749E-03	5.593E-02
1000	Sphere	0.776	7.640E-02	1.029E-02	6.611E-02
1000	Tetrahedron	0.776	8.652E-02	1.122E-02	7.530E-02
5000	Cylinder	3.879	3.968E+00	9.646E-02	3.872E+00
5000	Sphere	3.879	3.997E+00	9.093E-02	3.906E+00
5000	Tetrahedron	3.879	2.019E+00	1.242E-02	2.007E+00
10000	Cylinder	7.757	2.525E+00	1.496E-01	2.375E+00
10000	Sphere	7.757	2.344E+00	3.942E-02	2.305E+00
10000	Tetrahedron	7.757	6.655E-01	2.667E-04	6.651E-01

Table 3
Extinction efficiency, absorption, and scattering from water crystals.
The refractive index is 1.78+0.0024i and the wavelength is 0.81 cm (35 GHz)

Size Parameter (α) = $2\pi r/\lambda$					
Size (μm)	Shape	Size Param.	Q_ext	Q_abs	Q_sca
500	Cylinder	0.388	1.176E-02	1.621E-03	1.014E-02
500	Sphere	0.388	1.307E-02	1.735E-03	1.134E-02
500	Hexagon	0.388	1.310E-02	1.775E-03	1.133E-02
1000	Cylinder	0.776	1.998E-01	4.259E-02	1.572E-01
1000	Sphere	0.776	2.395E-01	4.572E-02	1.938E-01
1000	Hexagon	0.776	2.352E-01	4.658E-02	1.887E-01
5000	Cylinder	3.879	2.255E+00	4.736E-01	1.782E+00
5000	Sphere	3.879	3.585E+00	5.455E-01	3.040E+00
5000	Hexagon	3.879	3.408E+00	4.681E-01	2.940E+00
10000	Cylinder	7.757	2.025E+00	1.382E-01	1.887E+00
10000	Sphere	7.757	1.945E+00	5.826E-02	1.887E+00
10000	Hexagon	7.757	2.337E+00	1.111E-01	2.226E+00

Fig. 1

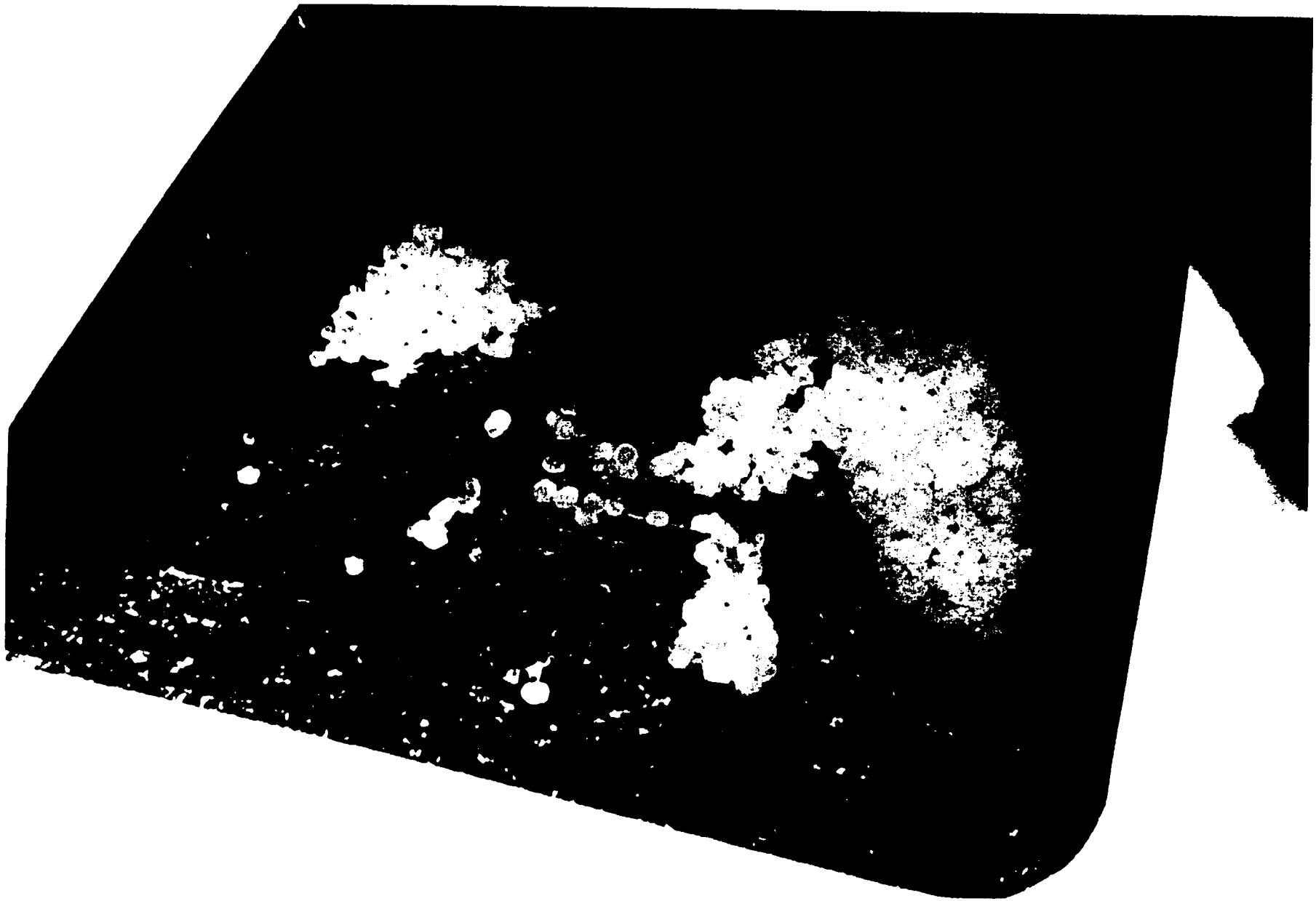

Fig 2

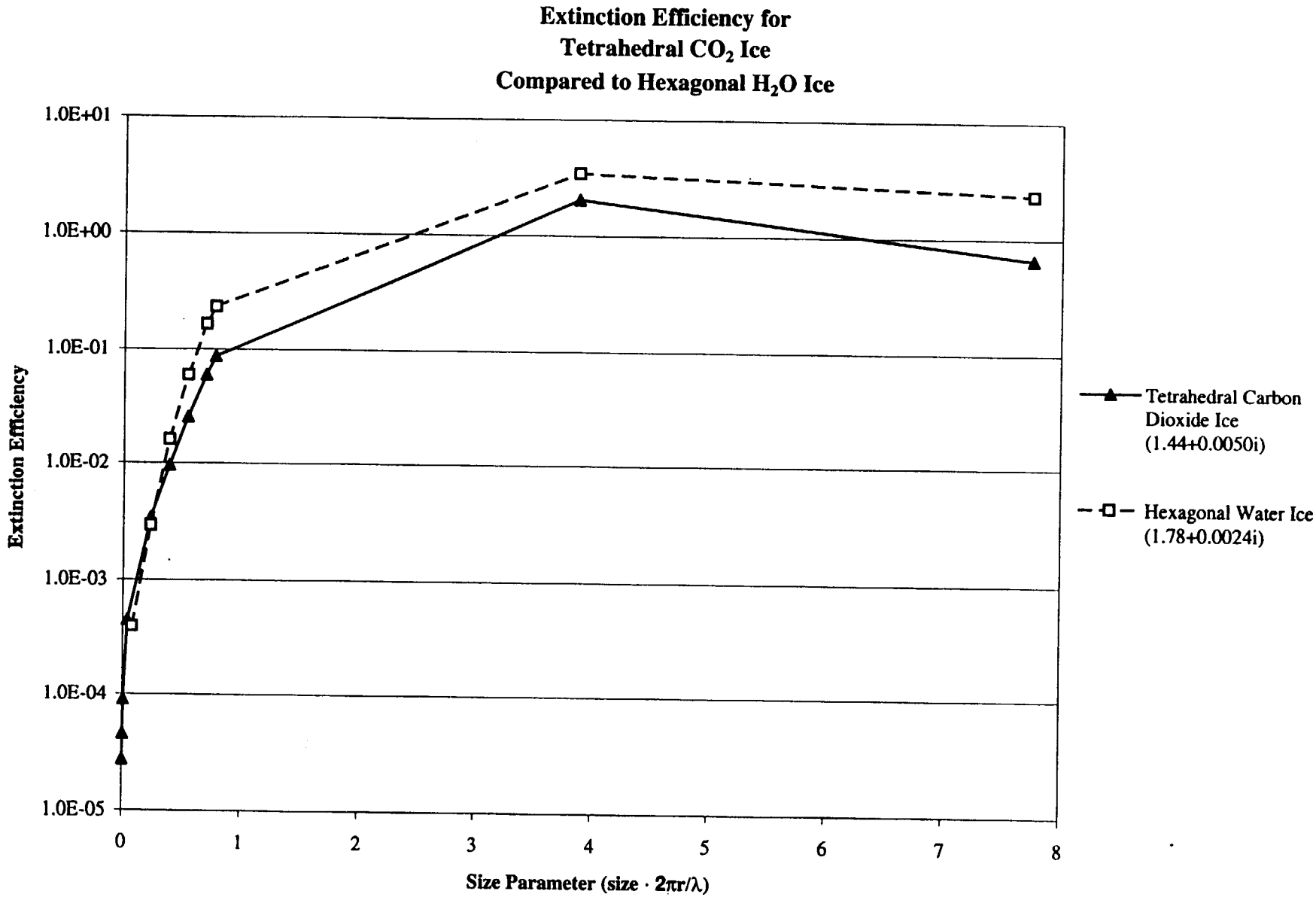
Extinction Efficiency for
Tetrahedral CO_2 Ice
Compared to Hexagonal H_2O Ice
1.0E+01
1.0E+00
1.0E-01
1.0E-02
1.0E-03
1.0E-04
1.0E-05
Extinction Efficiency
0
1
2
3
4
5
6
7
8
Size Parameter (size · 2πr/λ)
Tetrahedral Carbon Dioxide Ice (1.44+0.0050i)
Hexagonal Water Ice (1.78+0.0024i)

Fig. 3

35 GHz Brightness Temperature

Over Aluminum Plate (50 H)

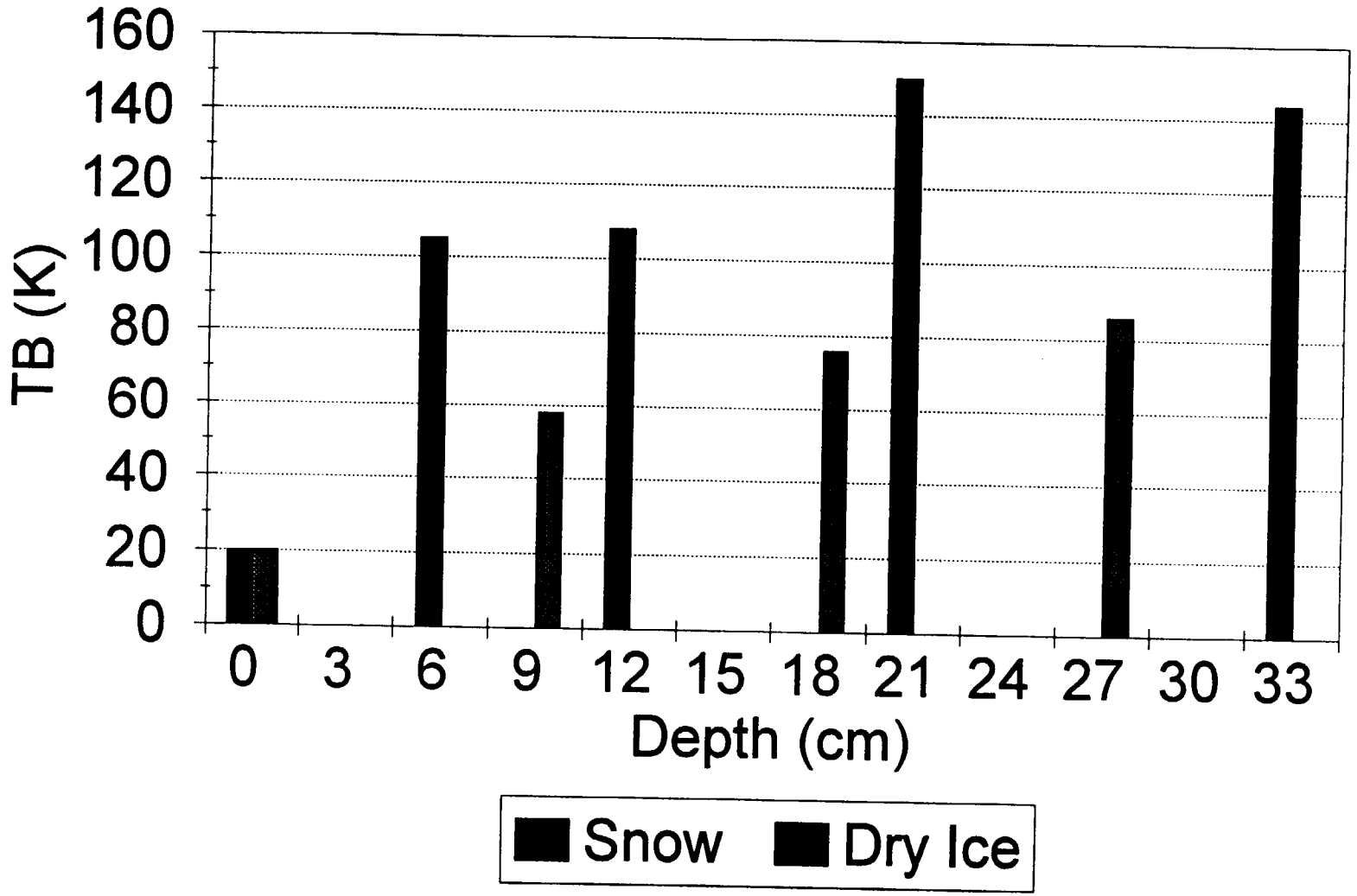

Fig. 4